On Half-Adders Based on Fusion of Signal Carriers: Excitation, Fluidics, and Electricity

Andrew Adamatzky
University of the West of England
Bristol, United Kingdom

Likely outcomes of a collision between two objects are annihilation, reflection, or fusion. We show how to construct a one-bit adder with patterns that fuse on impact. A fusion gate has two inputs and three outputs. When a signal is generated on a single input, the object propagates along its own output trajectory. When both inputs are active, the objects collide at a junction of input trajectories, fuse, and propagate along a dedicated output trajectory. Thus two outputs produce conjunction of one signal with negation of another signal, and the third output produces conjunction of input signals. By merging two outputs in one, we make a one-bit half-adder: one output is the conjunction of input signals; another output is the exclusive disjunction of the signals. We discuss blueprints of the half-adders realized with two types of physical signal carriers—wave fragments in excitable medium- and high-velocity jet streams. We also propose an electrical circuit analogous to a fusion half-adder. By running fusion half-adders in reverse, we find that despite realizing the same functions when in a straight mode, all devices implement different functions when their inputs are swapped with outputs.

1. Introduction

Unconventional computing is ninety-nine percent a conventional theory and only one percent novel computing substrates and devices. The majority of the novel computing devices are logical gates and circuits. Most circuits implemented in laboratory experiments so far are one-bit half-adders. A one-bit half-adder is a device with two inputs x and y and two outputs xy (carry out) and $x \oplus y$ (sum) (Figure 1).

Half-adders and their component gates are realized using enzymatic networks [1–5], photonic molecular devices [6–8], quantum logic inside a single molecule [9], molecular structural circuits [10, 11], acellular slime mold [12–15], nuclear magnetic resonance [16], ribosomes and mRNAs [17], peptide networks [18], and excitable chemical media [19–22]. In excitable chemical media, signal

https://doi.org/10.25088/ComplexSystems.25.3.237

carriers are excitation waves; the signals are modified via interaction between the excitation waves or wave fragments. The wave fragments colliding head-on annihilate. Not annihilation but merging happens when the wave fragments collide at an acute angle.

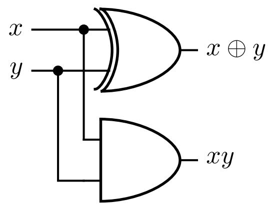

Figure 1. A logical diagram of a one-bit half-adder.

While designing reaction-diffusion computers, we found that when the excitation wave fragments in a thin-layer Belousov–Zhabotinsky (BZ) medium collide at an acute angle, they fuse into a single wave fragment that propagates along the bisector of the collision angle (Figure 2). Thus a fusion gate came into play [23]. If one of the wave fragments was not present, another wave fragment would move along its original trajectory. We interpret the presence and absence of wave fragments at a given site at a given time as True (1) and False (0) values of Boolean variables. Let a wave fragment traveling southeast represent value x, and a wave fragment traveling northeast represent value y. If $y = 0$, the corresponding wave fragment is not present. Then the wave fragment x continues its travel undisturbed. Thus its output trajectory represents $x\overline{y}$ (Figure 2). The output trajectory of undisturbed wave fragment y represents $\overline{x}y$. When both input variables are True, the wave fragments x and y collide and merge into a

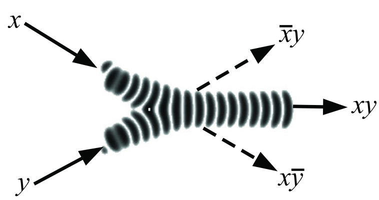

Figure 2. Time-lapse overlays of the fusion of two excitation wave fragments. One fragment is traveling from northwest to southeast, another fragment from southwest to northeast. The wave fragments collide and fuse into a new localized excitation traveling east. Note that these are not trains of waves but two single wave fragments recorded at regular time intervals and superimposed on the same image.

https://doi.org/10.25088/ComplexSystems.25.3.237

single wave fragment. This newly born wave fragment represents conjunction xy. The design works well, not just with BZ, but also with swarms of simulated or even living creatures, as we experimentally demonstrated in the prototype of the fusion gate made with soldier crabs [24].

If we go back into the 1950s–1960s, we find the fusion gate (Figure 2) was actually a rediscovery, although implemented in a novel substrate, of a jet stream AND gate, a key component of fluidic circuits [25, 26]. The fact that two gates were discovered with a 40-year interval prompted us to look more closely at the potential implementations of the fusion gate and binary arithmetic circuits made from it. This is the subject of the present paper. In Section 2, we discuss the design of gates made with an excitable chemical medium. Fluidic implementation of an adder is given in Section 3. Section 4 shows an electrical circuit analogous to BZ and fluidic adders. For several designs of half-adders proposed, when they are reversed, they produce different results from each other. This is discussed in Section 5.

2. Excitable Half-Adder

The BZ medium [27–30], a thin layer of a reaction-diffusion chemical system, can have non-excitable, sub-excitable, and excitable states. In an excitable thin-layer BZ system, a localized perturbation leads to a formation of omni-directional target waves or spiral excitation waves. A sub-excitable BZ medium responds to asymmetric local perturbations by producing traveling localized excitation wave fragments [31, 32]. The size and lifespan of an excitation wave fragment depend on the degree of the medium's excitability. The degree of excitability can be controlled by light [31, 33, 34]. Under the right conditions, the wave fragments conserve their shape and velocity vectors for extended periods of time.

Interaction of wave fragments shown in Figure 2 happens in a free space. The advantage of this is that literally any locus of space can be a signal conductor, causing wires to be momentary. The disadvantage is that due to the instability of wave fragments [31], which either expand or collapse, we must continuously monitor the size of the wave fragment and adjust the excitability of the medium to conserve the fragment's shape. A compromise can be achieved by geometrically constraining the excitation waves to excitable channels and allowing wave fragments to interact at sub-excitable junctions [35].

To illustrate the interaction between wave fragments, we use the two-variable Oregonator equation [36], adapted to a light-sensitive BZ reaction with applied illumination [37]:

$$
\begin{aligned}
\frac{\partial u}{\partial t} &= \frac{1}{\epsilon}\left(u - u^2 - (fv + \phi)\frac{u-q}{u+q}\right) + D_u \nabla^2 u \\
\frac{\partial v}{\partial t} &= u - v.
\end{aligned}
\tag{1}
$$

The variables u and v represent local concentrations of an activator, or an excitatory component of the BZ system, and an inhibitor, or a refractory component. The parameter ϵ relates to time scales of variables u and v, q is a scaling parameter depending on rates of activation and inhibition, and f is a stoichiometric coefficient. The constant ϕ is the rate of inhibitor production. In a light-sensitive BZ, ϕ represents the rate of inhibitor production proportional to the intensity of illumination in equation (1). We integrate the system using the Euler method with five-node Laplace operator, time step $\Delta t = 0.001$, and grid point spacing $\Delta x = 0.25$, $\epsilon = 0.02$, $f = 1.4$, $q = 0.002$. The parameter ϕ characterizes the excitability of the simulated medium. To generate the excitation wave fragments, we perturb the medium by square solid domains of excitation, 10×10 sites in state $u = 1.0$; if a different shape of perturbation was used, we indicate this in the captions of the figures. The medium is excitable and exhibits "classical" target waves when $\phi = 0.05$, and the medium is sub-excitable with propagating localizations, or wave fragments, when $\phi = 0.0766$. Time-lapse snapshots provided in the paper were recorded at every 150 time steps; we display sites with $u > 0.04$. The model has been repeatedly verified by us in experimental laboratory studies of the BZ system, and the satisfactory match between the model and the experiments has been demonstrated in [32, 38–40].

The geometry of the fusion gate F is shown in Figure 3(a). Channels are excitable. That is, if the channels' width and length were infinite, the excitation wave would be a growing circle. Thus we do not

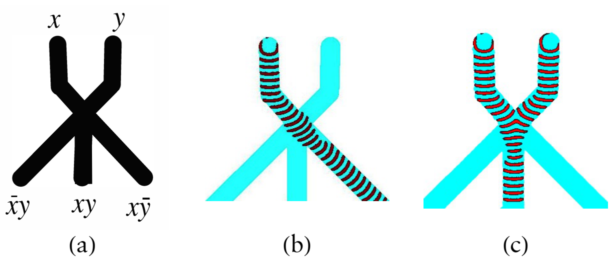

Figure 3. Fusion gate F. Channels are excitable; junctions are sub-excitable. (a) Scheme: inputs are x and y; outputs are xy, $\overline{x}y$, $x\overline{y}$. (b, c) Time-lapsed overlays of excitation waves. Note that these are not trains of waves but two single wave fragments recorded at regular time intervals and superimposed on the same image. (b) $x = 1$, $y = 0$. (c) $x = 1$, $y = 1$.

https://doi.org/10.25088/ComplexSystems.25.3.237

waste resources by controlling excitability when signals are in transit. If we kept a junction excitable, then excitation would propagate to all output channels. We keep the junction sub-excitable, and therefore wave fragments either propagate across the junction along their original trajectories, without spreading into branching channels (just one input is 1, Figure 3(c)), or collide and merge into a single wave fragment entering the central channel (two inputs are 1, Figure 3(e)).

By merging two lateral output channels $x\bar{y}$ and $\bar{x}y$ into a single output channel, we get a one-bit half-adder, gate A. A one-bit half-adder is a device with two inputs x and y and two outputs xy (carry out) and $x \oplus y$ (sum) (Figure 4(a)). It consists of two input channels a and

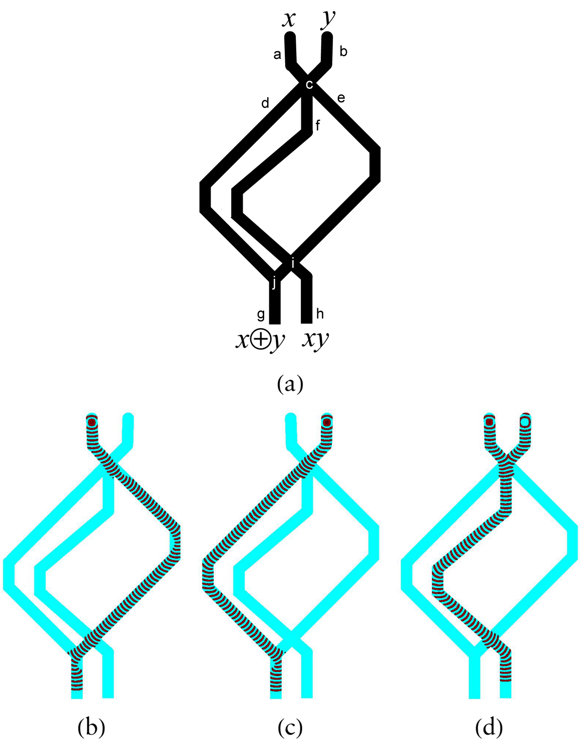

Figure 4. A one-bit half-adder, A_{BZ}-gate, filled with excitable chemical medium. (a) Scheme of the half-adder, gate A: a and b are input channels; g and h are output channels; d, e, and f are internal channels; and c, i, and j are junctions. Input variables x and y are fed into channels a and b; results $x \oplus y$ and xy are read from channels g and h. (b–d) Time-lapsed overlays of excitation waves propagation for inputs (b) $x = 1$, $y = 0$, (c) $x = 1$, $y = 0$, (d) $x = 1$, and $y = 1$. Sites of initial perturbation are visible as discs. Grid size is 500×790 nodes. These are time-lapsed snapshots of a single wave (b, c) or two waves merging into a single wave (d) recorded every 150^{th} step of numerical integration.

b and two output channels g and h. When gate A is filled with the BZ medium, we call this device A_{BZ}. The presence/absence of a wave fragment in an input/output channel of A_{BZ} symbolizes the logical True/False state of the input variable assigned to the channel. Synchronization of signal wave fragments is achieved geometrically: $|a| + |e| + |g| = |b| + |d| + |g| = |a| + |f| + |h|$, where $|\cdot|$ is a length of a channel (Figure 4(a)). Functioning of the half-adder A_{BZ} is shown in Figure 4(b–d). Two half-adders can be cascaded into a one-bit full adder; see details in [35].

3. Flueric Half-Adder

The BZ fusion gate proposed in [23] was in fact a rediscovery of the fluidic, or rather flueric, fusion gate. Signals in fluidic and flueric devices are represented by high-velocity jets issuing into the vented interaction region. Flueric devices are passive fluidic devices. They do not have any moving parts and do not change their shape to control a fluid [25, 26]. The flueric gates employ the phenomena of a wall attachment, jet interaction, and inertia [41]. The wall attachment of a jet happens due to a difference in space from the jet to the channel walls. The jet attracts air in the space between itself and one wall, and makes a vacuum in the space between itself and another wall [25].

The jet fusion gate shown in Figure 5 is among the first-ever fluidic devices made in the 1960s [25, 26]. It has two input ports A and B, one output port, and two vents. If pressure is applied only to one input, the jet goes into a vent. If both inputs are True (pressure is applied to both input channels), the opposing streams collide and merge into a single stream. The combined stream flows along the line that bisects the angle between the two intersecting jets and exits through the output port A and B (Figure 5). By converting vents into output channels, we can get a classical geometry of the fusion gate F (Figure 3(a)). By joining the vents into a single channel, we can produce a one-bit half-adder, gate A_F, similar to Figure 4(a). See the scheme of gate A_F functioning in Figure 6.

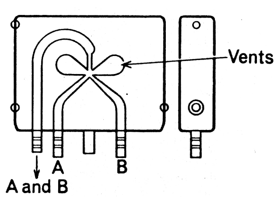

Figure 5. Diagram of an AND gate from [25].

https://doi.org/10.25088/ComplexSystems.25.3.237

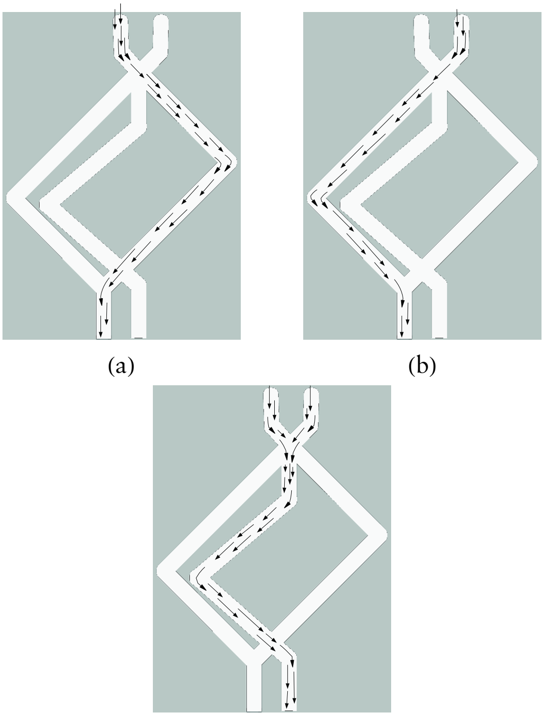

(a) (b) (c)

Figure 6. Flueric half-adder A_F based on geometry of A_{BZ}. (a) $x = 1$, $y = 0$. (b) $x = 0$, $y = 1$. (c) $x = 0$, $y = 1$. Jet streams are shown by arrows.

Joined vents seem to be unnecessary, as Hobbs demonstrated in 1963 [42]. Hobbs gate H is shown in Figure 7(a). Logical values are encoded by the presence of streams at specified channels. When only input $x = 1$, a power jet stream enters the gate via channel x. The stream is turned by the hook and follows channel p (Figure 7(b)). When only input $y = 1$, the power jet stream entering the gate via channel y locks on the left boundary wall of its channel and propagates along channel p (Figure 7(c)). If both inputs are True, streams entering x and y merge and follow channel q (Figure 7(d)). Thus the stream exiting channel p represents $p = x \oplus y$, and the stream exiting channel q represents $q = xy$.

Functioning of the Hobbs gate filled with the BZ medium instead of fluid, the H_{BZ} gate, is shown in Figure 8. For inputs $x = 1$ and $y = 0$, an excitation is initiated at the input lateral channel (Figure 8(a)). The wavefront propagates until the junction, enters the hook, reflects, and travels into the northwest output channel p. There the wave fragment is reflected again by the channel's wall and pro-

https://doi.org/10.25088/ComplexSystems.25.3.237

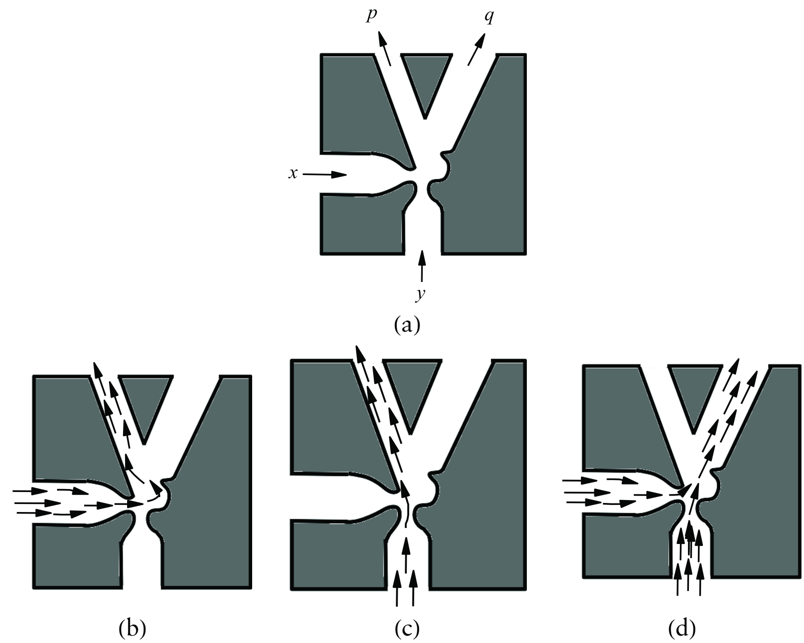

Figure 7. Hobbs gate *H*. (a) Structure of a hook-type fluidic half-adder. (b–d) Dynamics of fluid streams for inputs. (b) $x = 1$ and $y = 0$; (c) $x = 0$ and $y = 1$; (d) $x = 1$ and $y = 1$. Redrawn from [42].

ceeds to the output port. To represent input $x = 0$ and $y = 1$, we excite the BZ medium at the south input channel (Figure 8(b)). The excitation wave fragment travels straight, collides into the separation between output channels, and is reflected into the northwest output channel p. Excitation waves are generated in both input channels to represent inputs $x = 1$ and $y = 1$ (Figure 8(c–e)). The wave fragments collide at the junction and merge into a single wave fragment that propagates into the northeast output channel q. Even when wave fragments arrive at the collision site not exactly at the same moment, the resultant wave fragment travels into channel q. An example of "perfect" timing of the collision is shown in Figure 8(c). The wave fragment produced in a collision of wave fragments x and y partially collides with the northern part of the hook. A segment of the wave fragment that collided into the hook gets extinguished, while the intact segment of the wave fragment continues its travel and propagates along the middle of channel q. In the example shown in Figure 8(d), wave fragment x arrives at the junction earlier than wave fragment y. The delayed wave fragment y causes a substantial part of the newly formed wave fragment to collide into the hook; the remaining part is reflected into the northern wall of channel q (Figure 8(d)). Late arrival of wave fragment y also aberrates the trajectory of the output wave fragment (Figure 8(e)).

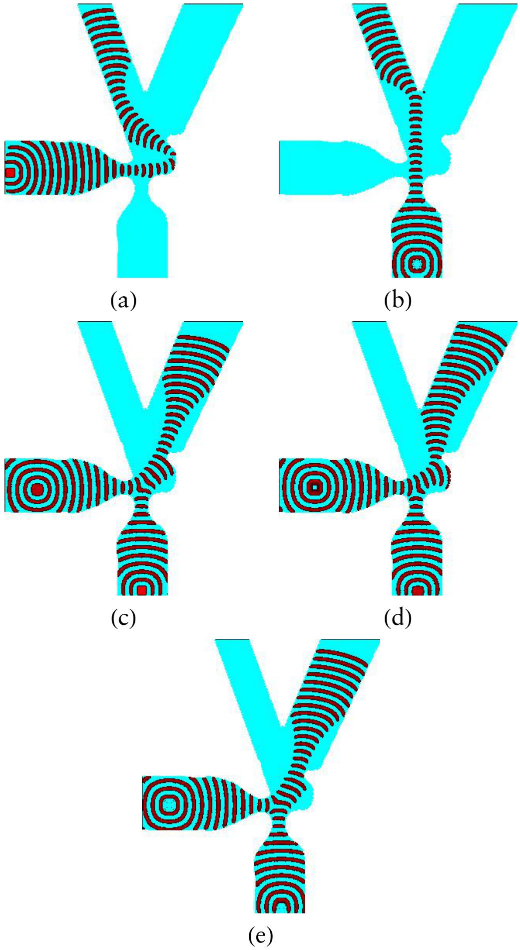

Figure 8. BZ in Hobbs gate, the H_{BZ} gate (Figure 7(a)). (a–e) Time-lapsed overlays of excitation waves for inputs. (a) $x = 0$, $y = 1$. (b) $x = 1$, $y = 0$. (c–e) $x = 1$, $y = 1$, an imperfect collision of wave fragments.

4. Electrical Half-Adder

Electrical current takes the path of least resistance. When designing a one-bit half-adder E where logical values are represented by electrical current, we take two input terminals and two output terminals. We should direct the current along the dedicated $x \oplus y$ terminal when

https://doi.org/10.25088/ComplexSystems.25.3.237

only one input terminal is connected to a current source (inputs $x = 1$ and $y = 0$ or $x = 0$ and $y = 1$), and along the xy terminal when both input terminals are connected to current sources (input $x = 1$, $y = 1$). This can be done with a fuse whose normal current rating is higher than the current going through one input terminal but less than the sum of currents via two input terminals. A scheme of E is shown in Figure 9(a). We use ideal electrical constant current sources s_1 and s_2. The sources have infinite source impedance and drive current through their terminals to the value of the specified current level e. Ideal resistor R has no parasitic effects. Fuse f has resistance much smaller than R and nominal rated current $e < i_f < 2e$. We assume logical input or output is True (1) when current through input or output terminal is nonzero. In practical circuits, that would mean the current exceeds some small threshold value ϵ.

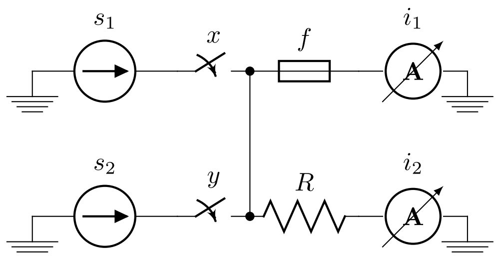

(a)

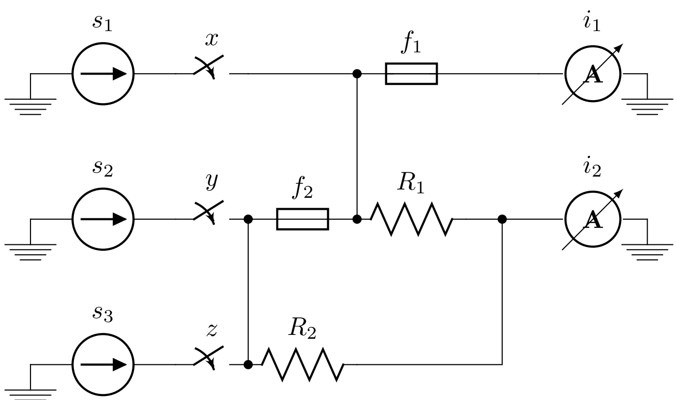

(b)

Figure 9. Schematic of: (a) one-bit half-adder, E-gate; and (b) full adder implemented with constant current sources s_1, s_2, s_3; resistors R; fuses f; and switches x and y.

If only switch x or switch y is On ($x = 1$ and $y = 0$ or $x = 0$ and $y = 1$), the current driven through the circuit is e. This current does

https://doi.org/10.25088/ComplexSystems.25.3.237

not melt the fuse f and, because the resistance of the fuse f is much less than that of R, the current travels along a path from x or y to f, then to ammeter i_1. When both switches x and y are On, the current through the circuit is $2e$. The current melts the fuse f and then travels along the route (s_1, s_2) to R and i_2. Thus current on the output terminal i_1 represents disjunction $x \oplus y$ of input variables and the output terminal i_2—conjunction xy. The analogous half-adder can be interfaced with digital circuits. Switches x and y are binary. Terminals i_1 and i_2 can be connected to a converter from a continuous quantity input to a one-bit digital output, for example, standard IEEE 1164, by specifying the conversion threshold of the current.

The half-adder E is modified to a full adder as shown in Figure 9(b). If only one input is True, the current goes along a path including only fuses; for example, for input $x = 0$, $y = 0$, $z = 1$, the current path is s_3 to x, to f_2, to f_1, to i_1. If two input terminals are True, the current goes from each source along its unique shortest path until merger. For example, for input $x = 1$, $y = 0$, $z = 1$, the current propagates from s_1 to x and from s_3 to z via fuse f to the junction point. After the junction point, the current becomes $2e$ and the fuse is blown, and then the current follows the path via R_1 to i_2. Ammeter i_1 shows nonzero current e only if exactly one of the switches is On. Ammeter i_2 shows nonzero current if two or three switches are On; the current shown is $n \cdot e$, where n is a number of switches in position On. Terminal i_1 represents $x \oplus y \oplus z$. Terminal i_2 represents $xy + z(x \oplus y)$.

5. Reversing Circuits

What would happen if we swapped inputs with outputs in the BZ, flueric, and electrical half-adders? We call a gate G reversed G^* if its original inputs become outputs and outputs become inputs.

The reversed BZ gate (Figure 4(a)) always produces False outputs, $A^*_{\mathrm{BZ}}(p, q) = \langle 0, 0 \rangle$. This is because a medium at the junctions j and c is sub-excitable (see labels in Figure 4(a)). Thus, when input is generated only in channel g, the wave fragment collides into the intersection at junction j and gets extinguished. Even if the excitation wave did not die at junction j but split into two waves, propagating along channels d and e, the waves would collide with each other at junction c and annihilate. If input is generated only in channel h, then the excitation wave propagates along channel f and reaches junction c. The medium in junction c is sub-excitable: the waves collide into the separation between channels a and b and extinguish. When inputs are activated in both channels g and h, the wave traveling from g be-

https://doi.org/10.25088/ComplexSystems.25.3.237

comes extinguished at junction j, and the wave traveling along channels h and f becomes extinguished at junction c.

Reversed Hobbs gate H^* is shown in Figure 10. Assume ports p and q (Figure 7(a)) are inputs. When $p = 1$ and $q = 0$, the jet stream entering channel p interacts with the cavity of the hook structure and gets diverted into the output port x (Figure 10(a)). When $p = 0$ and $q = 1$, the jet stream entering channel q is deflected by the upper part of the hook structure and diverted into channel p (Figure 10(b)). When both inputs are activated ($p = 1$ and $q = 1$), the jet streams merge into a single stream that enters output channel y (Figure 10(d)). Thus, the reversed Hobbs gate implements operation $H^*(p, q) = \langle p\overline{q}, pq \rangle$.

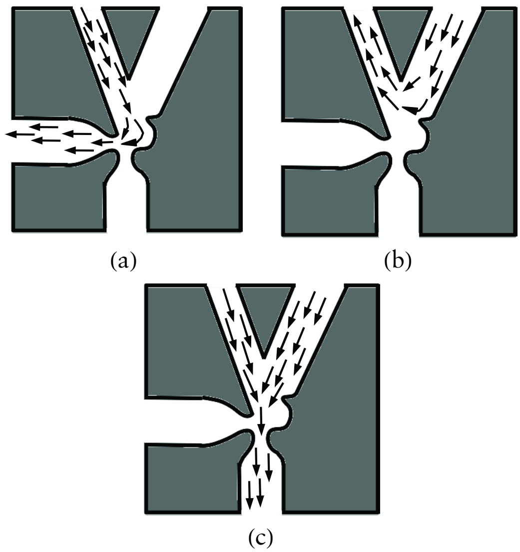

Figure 10. Reversed Hobbs gate, or H^* gate, for inputs (a) $p = 1$, $q = 0$; (b) $p = 0$, $q = 1$; and (c) $p = 1$, $q = 1$.

Swapping input and output ports in a flueric half-adder (Figure 6) A_F^* makes mapping indeterministic. This is because when only one input is activated, the stream meets a binary branching point at least once. At that branching site, the stream either splits into two streams, if jet energy is moderate, and then follows both branches, or attaches itself arbitrarily to one of the output branches if jet energy is high.

Hobbs gate with reversed inputs and filled with BZ medium implements operation $H_{BZ}^*(p, q) = \langle 0, p + q \rangle$ because for all nonzero inputs the resultant wave fragments travel into output channel q as demonstrated by modeling results in Figure 11.

https://doi.org/10.25088/ComplexSystems.25.3.237

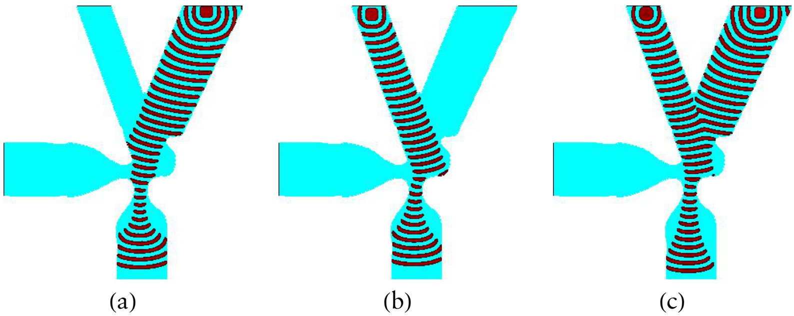

Figure 11. Reversed BZ implementation of Hobbs gate, H^*_{BZ} gate, for inputs (a) $x = 0$, $y = 1$; (b) $x = 1$, $y = 0$; (c) $x = 1$, $y = 1$.

The reversed circuit E, gate E^*, is shown in Figure 12. If switch p is On, the current flows along the fuse f, spreads along the short, and reaches ammeters i_1 and i_2. If switch q is On, the current flows along the resistor R, spreads along the short, and reaches both ammeters. If both switches are On, the current again propagates toward both outputs. Thus, we have $E^*(p, q) = \langle p + q, p + q \rangle$; each output of the reversed electrical half-adder is a disjunction of inputs. Operations implemented by all reversed gates are summarized in Table 1.

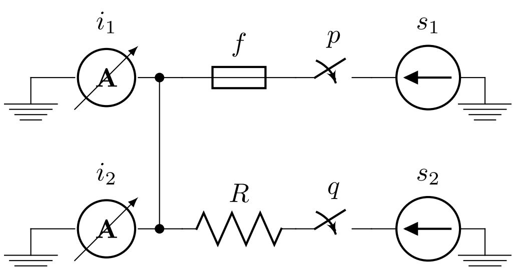

Figure 12. Reversed electronic circuit, E^*-gate.

Gate	Operation	Medium
$A^*_{BZ}(p, q) =$	$\langle 0, 0 \rangle$	excitable media
$A^*_F(p, q) =$	$\langle ?, ? \rangle$	fluid streams
$H^*(p, q) =$	$\langle p\overline{q}, pq \rangle$	fluid streams
$H^*_{BZ}(p, q) =$	$\langle 0, p + q \rangle$	excitable media
$E^*(p, q) =$	$\langle p + q, p + q \rangle$	electricity

Table 1. Reversed half-adders.

https://doi.org/10.25088/ComplexSystems.25.3.237

6. Discussion

Half-adder implementations via fusion of signals in three different substrates—excitable chemical media, fluidic system, and electrical circuit—show the same degree of structural complexity. Gate *A* has two junctions (intersection *i* of channels does not count because signals never meet there). Gate *H* has one junction and one reflector (the hook structure). Circuit *E* consists of one fuse and one resistor. The gates with an excitable system and jet streams employ physical interaction of patterns representing signals and their reflection by impenetrable barriers. The electrical circuit uses a link that becomes nonconductive when the strength of the input signal increases. The hook structure in Hobbs gate *H* is functionally analogous to a fuse in circuit *E*: the fuse blows when both sources of current are On, and the hook does not affect jet streams when they merge in a single stream.

The half-adders implement different sets of functions when they are reversed, that is, inputs are swapped with outputs. Reversed gate *A* produces constant False or indeterministic outputs. Reversed gate *H* working on jet streams implements conjunction of one input with negation of another on one output and conjunction of inputs on another output. Reversed gate *H* filled with an excitable chemical medium produces constant False on one output and disjunction of inputs on another. Reversed electrical circuit *E* produces conjunction of input signals on both outputs.

To make fusion-based gates cascadable, we must preserve the physical quantity of signals. Gates implemented in an excitable chemical medium preserve the quantity of signals: when two wave fragments fuse, the newly formed wave fragment, when it leaves the output port, has the same shape and level of excitation as each of the input wave fragments. Flueric and electrical gates do not preserve the quantity of signals. Two merging jet streams are stronger than each of the input streams. Electrical current on the output terminal doubles (subject to resistance of the fuse) when both input terminals are active. These issues are not critical, however, because by using technology converters, the signals can be normalized to their original states.

References

[1] M. N. Stojanovic and D. Stefanovic, "Deoxyribozyme-Based Half-Adder," *Journal of the American Chemical Society*, **125**(22), 2003 pp. 6673–6676. doi:10.1021/ja0296632.

[2] H. Lederman, J. Macdonald, D. Stefanovic, and M. N. Stojanovic, "Deoxyribozyme-Based Three-Input Logic Gates and Construction of a Molecular Full Adder," *Biochemistry*, **45**(4), 2006 pp. 1194–1199. doi:10.1021/bi051871u.

[3] R. Baron, O. Lioubashevski, E. Katz, T. Niazov, and I. Willner, "Elementary Arithmetic Operations by Enzymes: A Model for Metabolic Pathway Based Computing," *Angewandte Chemie International Edition*, **45**(10), 2006 pp. 1572–1576. doi:10.1002/anie.200503314.

[4] E. Katz and V. Privman, "Enzyme-Based Logic Systems for Information Processing," *Chemical Society Reviews*, **39**(5), 2010 pp. 1835–1857. doi:10.1039/b806038j.

[5] M. Ikeda, T. Tanida, T. Yoshii, K. Kurotani, S. Onogi, K. Urayama, and I. Hamachi, "Installing Logic-Gate Responses to a Variety of Biological Substances in Supramolecular Hydrogel–Enzyme Hybrids," *Nature Chemistry*, **6**(6), 2014 pp. 511–518. doi:10.1038/nchem.1937.

[6] J. Andréasson, G. Kodis, Y. Terazono, P. A. Liddell, S. Bandyopadhyay, R. H. Mitchell, T. A. Moore, A. L. Moore, and D. Gust, "Molecule-Based Photonically Switched Half-Adder," *Journal of the American Chemical Society*, **126**(49), 2004 pp. 15926–15927. doi:10.1021/ja045577l.

[7] J. Andréasson, S. D. Straight, G. Kodis, C.-D. Park, M. Hambourger, M. Gervaldo, B. Albinsson, T. A. Moore, A. L. Moore, and D. Gust, "All-Photonic Molecular Half-Adder," *Journal of the American Chemical Society*, **128**(50), 2006 pp. 16259–16265. doi:10.1021/ja0654579.

[8] X. Guo, D. Zhang, G. Zhang, and D. Zhu, "Monomolecular Logic: 'Half-Adder' Based on Multistate/Multifunctional Photochromic Spiropyrans," *The Journal of Physical Chemistry B*, **108**(32), 2004 pp. 11942–11945. doi:10.1021/jp047706q.

[9] I. Duchemin and C. Joachim, "A Quantum Digital Half Adder Inside a Single Molecule," *Chemical Physics Letters*, **406**(1–3), 2005 pp. 167–172. doi:10.1016/j.cplett.2005.02.090.

[10] J. C. Ellenbogen and J. C. Love, "Architectures for Molecular Electronic Computers: I. Logic Structures and an Adder Designed from Molecular Electronic Diodes," *Proceedings of the IEEE*, **88**(3), 2000 pp. 386–426. doi:10.1109/5.838115.

[11] S. J. Langford and T. Yann, "Molecular Logic: A Half-Subtractor Based on Tetraphenylporphyrin," *Journal of the American Chemical Society*, **125**(37), 2003 pp. 11198–11199. doi:10.1021/ja036909+.

[12] S. Tsuda, M. Aono, and Y.-P. Gunji, "Robust and Emergent *Physarum* Logical-Computing," *Biosystems*, **73**(1), 2004 pp. 45–55. doi:10.1016/j.biosystems.2003.08.001.

[13] A. Adamatzky, "Slime Mould Logical Gates: Exploring Ballistic Approach." arxiv.org/abs/1005.2301.

[14] J. Jones and A. Adamatzky, "Towards *Physarum* Binary Adders," *Biosystems*, **101**(1), 2010 pp. 51–58. doi:10.1016/j.biosystems.2010.04.005.

[15] J. G. H. Whiting, B. P. J. de Lacy Costello, and A. Adamatzky, "Slime Mould Logic Gates Based on Frequency Changes of Electrical Potential Oscillation," *Biosystems*, **124**, 2014 pp. 21–25. doi:10.1016/j.biosystems.2014.08.001.

[16] M. Roselló-Merino, M. Bechmann, A. Sebald, and S. Stepney, "Classical Computing in Nuclear Magnetic Resonance," *International Journal of Unconventional Computing*, **6**(3–4), 2009 pp. 163–195

[17] O. Rackham and J. W. Chin, "Cellular Logic with Orthogonal Ribosomes," *Journal of the American Chemical Society*, **127**(50), 2005 pp. 17584–17585. doi:10.1021/ja055338d.

[18] G. Ashkenasy and M. R. Ghadiri, "Boolean Logic Functions of a Synthetic Peptide Network," *Journal of the American Chemical Society*, **126**(36), 2004 pp. 11140–11141. doi:10.1021/ja046745c.

[19] J. Gorecki, K. Yoshikawa, and Y. Igarashi, "On Chemical Reactors That Can Count," *The Journal of Physical Chemistry A*, **107**(10), 2003 pp. 1664–1669. doi:10.1021/jp021041f.

[20] J. N. Gorecka, J. Gorecki, and Y. Igarashi, "On the Simplest Chemical Signal Diodes Constructed with an Excitable Medium," *International Journal of Unconventional Computing*, **5**(2), 2009 pp. 129–143.

[21] B. de Lacy Costello, A. Adamatzky, I. Jahan, and L. Zhang, "Towards Constructing One-Bit Binary Adder in Excitable Chemical Medium," *Chemical Physics*, **381**(1–3), 2011 pp. 88–99. doi:10.1016/j.chemphys.2011.01.014.

[22] J. Gorecki, J. N. Gorecka, and A. Adamatzky, "Information Coding with Frequency of Oscillations in Belousov–Zhabotinsky Encapsulated Disks," *Physical Review E*, **89**(4), 2014 042910. doi:10.1103/PhysRevE.89.042910.

[23] A. Adamatzky, "Collision-Based Computing in Belousov–Zhabotinsky Medium," *Chaos, Solitons & Fractals*, **21**(5), 2004 pp. 1259–1264. doi:10.1016/j.chaos.2003.12.068.

[24] Y.-P. Gunji, Y. Nishiyama, and A. Adamatzky, "Robust Soldier Crab Ball Gate," *Complex Systems*, **20**(2), 2011 pp. 93–104. http://www.complex-systems.com/pdf/20-2-2.pdf.

[25] M. J. Moylan, *Fluid Logic in Simple Terms*, Brighton: The Machinery Publishing Co. Ltd., 1968.

[26] A. Conway (ed.), *A Guide to Fluidics*, New York: American Elsevier, 1971.

[27] B. P. Belousov, "A Periodic Reaction and Its Mechanism," in *Collection of Short Papers on Radiation Medicine for 1958*, Moscow: Medgiz Publishers, 1959 p. 1.

[28] A. M. Zhabotinsky, “Periodic Course of the Oxidation of Malonic Acid in Solution (A Study on the Kinetics of Belousov’s Reaction),” *Biofizika*, **9**, 1964 pp. 306–311.

[29] A. T. Winfree, “The Prehistory of the Belousov–Zhabotinsky Oscillator,” *Journal of Chemical Education*, **61**(8), 1984 p. 661–663. doi:10.1021/ed061p661.

[30] R. Kapral and K. Showalter (eds.), *Chemical Waves and Patterns*, Dordrecht: Kluwer Academic Publishers, 1995. doi:10.1007/978-94-011-1156-0.

[31] I. Sendiña-Nadal, E. Mihaliuk, J. Wang, V. Pérez-Muñuzuri, and K. Showalter, “Wave Propagation in Subexcitable Media with Periodically Modulated Excitability,” *Physical Review Letters*, **86**(8), 2001 pp. 1646–1649. doi:10.1103/PhysRevLett.86.1646.

[32] B. de Lacy Costello, R. Toth, C. Stone, A. Adamatzky, and L. Bull, “Implementation of Glider Guns in the Light-Sensitive Belousov–Zhabotinsky Medium,” *Physical Review E*, **79**(2), 2009 026114. doi:10.1103/PhysRevE.79.026114.

[33] L. Kuhnert, “A New Optical Photochemical Memory Device in a Light-Sensitive Chemical Active Medium,” *Nature*, **319**(6052), 1986 pp. 393–394. doi:10.1038/319393a0.

[34] A. Adamatzky, “If BZ Medium Did Spanning Trees These Would Be the Same Trees as *Physarum* Built,” *Physics Letters A*, **373**(10), 2009 pp. 952–956. doi:10.1016/j.physleta.2008.12.070.

[35] A. Adamatzky, “Binary Full Adder, Made of Fusion Gates, in a Subexcitable Belousov–Zhabotinsky System,” *Physical Review E*, **92**(3), 2015 032811. doi:10.1103/PhysRevE.92.032811.

[36] R. J. Field and R. M. Noyes, “Oscillations in Chemical Systems: IV. Limit Cycle Behavior in a Model of a Real Chemical Reaction,” *The Journal of Chemical Physics*, **60**(5), 1974 pp. 1877–1884. doi:10.1063/1.1681288.

[37] V. Beato and H. Engel, “Pulse Propagation in a Model for the Photosensitive Belousov–Zhabotinsky Reaction with External Noise,” in *Proceedings SPIE 5114, Noise in Complex Systems and Stochastic Dynamics*, Santa Fe, 2003 (L. Schimansky-Geier, D. Abbott, A. Neiman, and C. Van den Broeck, eds.) Bellingham, WA: SPIE, 2003 pp. 353–362. doi:10.1117/12.490183.

[38] A. Adamatzky and B. de Lacy Costello, “Binary Collisions between Wave-Fragments in a Sub-excitable Belousov–Zhabotinsky Medium,” *Chaos, Solitons & Fractals*, **34**(2), 2007 pp. 307–315. doi:10.1016/j.chaos.2006.03.095.

[39] R. Toth, C. Stone, B. de Lacy Costello, A. Adamatzky, and L. Bull, "Simple Collision-Based Chemical Logic Gates with Adaptive Computing," in *Theoretical and Technological Advancements in Nanotechnology and Molecular Computation: Interdisciplinary Gains* (B. MacLennan, ed.), Hershey, PA: Information Science Reference, 2010 p. 162. doi:10.4018/978-1-60960-186-7.ch011.

[40] A. Adamatzky, B. de Lacy Costello, L. Bull, and J. Holley, "Towards Arithmetic Circuits in Sub-excitable Chemical Media," *Israel Journal of Chemistry*, **51**(1), 2011 pp. 56–66. doi:10.1002/ijch.201000046.

[41] C. A. Belsterling, *Fluidic Systems Design*, New York: Wiley-Interscience, 1971.

[42] E. V. Hobbs, *Fluid Amplification. 9. Logic Elements*, Technical Report, Harry Diamond Laboratories TR-1114, 1963.